Available online at www.sciencedirect.com

SCIENCE DIRECT

International Journal of Heat and Mass Transfer 49 (2006) 1679–1684

International Journal of HEAT and MASS TRANSFER

www.elsevier.com/locate/ijhmt

Application of the time discontinuous Galerkin finite element method to heat wave simulation

Wenhua Wu, Xikui Li *

The State Key Laboratory for Structural Analysis of Industrial Equipment, Dalian University of Technology, Dalian 116024, China

Received 31 March 2005; received in revised form 24 October 2005
Available online 20 December 2005

Abstract

This paper deals with the numerical simulation of heat wave propagation in the medium subjected to different kinds of heat source, particularly heat impulse. The discontinuous Galerkin finite element method (DGFEM) proposed for the stress wave propagation in solids [X.K. Li, D.M. Yao, R.W. Lewis, A discontinuous Galerkin finite element method for dynamic and wave propagation problems in non-linear solids and saturated porous media. Int. J. Numer. Meth. Eng. 57 (2003) 1775–1800] is extended to numerically solve for the non-Fourier heat transport equation constructed according to the CV model [C. Cattaneo, A form of heat-conduction equation which eliminates the paradox of instantaneous propagation, Compute Rendus 247 (1958) 431–433; P. Vernotte, Les paradoxes de la theorie continue de l'equation de la chaleur, Compute Rendus 246 (1958) 3154–3155]. Temperature and its time-derivative are chosen as primitive variables defined at each FE node. The main distinct characteristic of the proposed DGFEM is that the specific P3–P1 interpolation approximation, which uses piecewise cubic (Hermite's polynomial) and linear interpolations for both temperature and its time-derivative, respectively, in the time domain is particularly proposed. As a consequence the continuity of temperature at each discrete time instant is exactly ensured, whereas discontinuity of the time-derivative of temperature at discrete time levels remains. Numerical results illustrate good performance of the present method in the numerical simulation of heat wave propagation in eliminating spurious numerical oscillations and in providing more accurate solutions in the time domain.

Keywords: Time discontinuous; Heat wave; Non-Fourier effect; DGFEM; The CV model

1. Introduction

Nowadays, the non-Fourier heat-conduction phenomenon has attracted more attentions in engineering sciences, especially in the use of heat sources such as lasers and microwaves. Because of the characteristic of such heat sources applied with extremely short duration or very high frequency or quite high heat flux densities, it brings the inaccuracy of the classical Fourier heat diffusion theory.

The classical parabolic model of heat-conduction based on the Fourier law of heat propagation provides acceptable results for most engineering applications. However, it fails to properly capture the heat wave behavior characterized with the hyperbolic nature, particularly discontinuities or sharp gradients of the solution due to propagating impulsive heat waves in the medium subjected to the heat impulse with heat action time shorter than a pico-, even a femto-second.

Cattaneo [2] and Vernotto [3] developed their versions of the CV model independently, in which the relaxation of heat flux, i.e. the non-Fourier effect, is introduced to upgrade the classical Fourier heat-conduction equation to the non-Fourier heat-conduction equation for the model given below

$$q + \tau_0 \frac{\partial}{\partial t} q = -\lambda \nabla T \tag{1}$$

where q is heat flux, T temperature, λ the thermal conductivity and τ_0 the relaxation time (non-negative constant). If the relaxation time $\tau_0 = 0$, the heat flux law of the CV

* Corresponding author. Tel./fax: +86 411 84709186.
E-mail address: xikuili@dlut.edu.cn (X. Li).

0017-9310/$ - see front matter © 2005 Elsevier Ltd. All rights reserved.
doi:10.1016/j.ijheatmasstransfer.2005.10.025

Nomenclature

q	heat flux	$\mathbf{T}$	temperature vector
T	temperature	$\mathbf{v}$	temporal derivative vector of temperature
t	time	$\mathbf{w}$	time-jump function
I	partition of time domain		
a	thermal diffusivity	*Greek symbols*	
N, M	Hermite interpolation function	τ_0	relaxation time
$\mathbf{M}$, $\mathbf{C}$	generalized mass matrix	λ	thermal conductivity
$\mathbf{K}$	stiffness matrix	λ_i	function
$\mathbf{Q}$	heat source vector		

model defined by Eq. (1) reduces to the classical Fourier's model for heat conduction. Inserting Eq. (1) into the energy conservation equation, the hyperbolic heat transport equation, including source term, takes the form

$$a\nabla^2 T = \frac{\partial T}{\partial t} + \tau_0 \frac{\partial^2 T}{\partial t^2} + Q(x,t) \tag{2}$$

where a is thermal diffusivity, Q source term. $\sqrt{a/\tau_0}$ the propagation speed of temperature wave.

Various solution schemes for governing equation (2) with different initial and boundary conditions can be browsed in literatures. Among them are the finite difference method and the finite element method. Duhamel [4] presented a finite integral transform method for heat wave conduction problems. Casas-Vazquez and Jou [5] proposed a backward difference method in space that is capable of modelling ultra-fast laser heating process. There exist many other different versions of the finite integral method and finite difference method, such as those given in [6,7].

The finite element method has been widely accepted as one of most general and effective approaches available for the numerical solutions of most of engineering problems. The standard (continuous) Galerkin finite element method (CGFEM) combined with different types of direct time integration procedures, such as the Newmark family method, has been used to numerically analyze non-Fourier heat-conduction problems. The primary unknown variable, i.e. temperature, and its temporal derivative are assumed continuous in the discretization in the time domain. However, CGFEM generally fails to properly capture discontinuities or sharp gradients of the solution due to propagating impulsive waves in space and is incapable of filtering out the effects of spurious high modes and controlling spurious numerical oscillation.

Tamma et al. [8–10] devoted many efforts in getting rid of the spurious oscillation with success. They developed the γ-family method with the three coefficients, in which a smooth procedure was introduced to filter out the effects of spurious high modes. The disadvantage of the method is that one of the coefficients γ_3 used in the smooth procedure has to be adjusted case by case to stabilize the solution procedure and to control the spurious oscillation for the non-classical problems.

The present work extended the new version of the time discontinuous Galerkin finite element method (DGFEM) developed by Li et al. [1] to the heat wave propagation problem. The essential feature of the proposed DGFEM distinct from the previous versions of DGFEM is its P3–P1 interpolation approximations, i.e. the primary variable (the displacement vector in the solid mechanics and temperature in the heat transfer problems) and its temporal derivative are approximately interpolated by the Hermite (i.e. the third-order polynomial, P3) and the linear (i.e. the first-order polynomial, P1) interpolation functions in the time domain, respectively. In comparison with CGFEM to solve time dependent problems, the primary unknown variable i.e. temperature and its temporal derivative in DGFEM are assumed to be discontinuous at each of discrete time instants in their discretization in the time domain. The relaxation of restrictions on continuity of the primary variable and its temporal derivative provides a mechanism to filter the spurious oscillations without the need of introduction of any artificial coefficients and then much more accurate solutions than does CGFEM using the Newmark method as the same time step size is used. Even though, on the other hand, DGFEM formulations typically lead to a system of coupled equations with four times larger than that generated by CGFEM using the Newmark method. Nevertheless it is indicated that [1] DGFEM is three-order accurate and may use a larger time step size than CGFEM, in addition, the explicit algorithm of proposed DGFEM is used to avoid directly solving the system of coupled simultaneous equations. Hence, the total computational cost of DGFEM may be still comparable with that of CGFEM.

2. The algorithm of the DG method in time domain

With the traditional finite element method, Eq. (2) can be discretized in spatial domain Ω and expressed as

$$\mathbf{M}\ddot{\mathbf{T}}(t) + \mathbf{C}\dot{\mathbf{T}}(t) + \mathbf{K}\mathbf{T}(t) = \mathbf{Q}(t), \quad t \in I = (0, T) \tag{3}$$

$$\mathbf{M} = \int_\Omega N^{\mathrm{T}} \tau_0 N \,\mathrm{d}\Omega, \quad \mathbf{C} = \int_\Omega N^{\mathrm{T}} N \,\mathrm{d}\Omega$$

$$\mathbf{K} = \int_\Omega \nabla N^{\mathrm{T}} \alpha \nabla N \,\mathrm{d}\Omega, \quad \mathbf{Q} = \int_{\Omega_f} N^{\mathrm{T}} Q(t) \,\mathrm{d}\Omega_f$$

where $\mathbf{M}$ and $\mathbf{C}$ can be regarded as the generalized mass matrices, $\mathbf{K}$ is the stiffness matrix, $\mathbf{Q}$ is the vector of heat source, $\mathbf{T}, \dot{\mathbf{T}}, \ddot{\mathbf{T}}$ are the temperature and its first-order and second-order temporal derivatives, respectively. Ω_f is the domain of heat flux. I is the time domain. Let $I = (0, T)$ be a partition of the time domain, having the form: $0 < t_1 < \cdots < t_n < t_{n+1} < \cdots < t_N = T$. DGFEM permits discontinuities of functions at discretized time levels. For a typical time instant t_n, the temporal jump of the function $w(t_n) = w_n$ can be expressed as

$$[[\mathbf{w}_n]] = \mathbf{w}(t_n^+) - \mathbf{w}(t_n^-) \tag{4}$$

where

$$\mathbf{w}(t_n^\pm) = \lim_{\varepsilon\to 0^\pm} \mathbf{w}(t_n + \varepsilon) \tag{5}$$

Denote $I_n = (t_n^-, t_{n+1}^-)$ a typical incremental time step with the step size $\Delta t = t_{n+1} - t_n$. The primary unknown vector (the global nodal temperature vector) of the semi-discretized equation (3) at time $t \in [t_n, t_{n+1}]$ in the current time step I_n is interpolated by using the third-order Hermite (P3) time shape functions as

$$\mathbf{T}(t) = \mathbf{T}_n^+ N_1(t) + \mathbf{T}_{n+1}^- N_2(t) + \mathbf{v}_n^+ M_1(t) + \mathbf{v}_{n+1}^- M_2(t) \tag{6}$$

where $\mathbf{T}_n^+, \mathbf{T}_{n+1}^-, \mathbf{v}_n^+, \mathbf{v}_{n+1}^-$ stand for the global nodal values of temperature and its time-derivative at times t_n^+, t_{n+1}^-, respectively. For clarity Eq. (6) is rewritten with the omission of the superscripts of the vectors $\mathbf{T}_n$, $\mathbf{T}_{n+1}$, $\mathbf{v}_n$, $\mathbf{v}_{n+1}$ and the time variable t in the equation as

$$\mathbf{T} = \mathbf{T}_n N_1 + \mathbf{T}_{n+1} N_2 + \mathbf{v}_n M_1 + \mathbf{v}_{n+1} M_2 \tag{7}$$

It is assumed for the current time step that the global nodal values of temperature and its time-derivative, i.e. $\mathbf{T}_n^-, \mathbf{v}_n^-$ at time t_n^- have been determined at the end of the previous time step. The Hermite (P3) interpolation functions used in Eq. (7) are given as

$$\begin{aligned} &N_1 = N_1(t) = \lambda_1^2(\lambda_1 + 3\lambda_2); \quad N_2 = N_2(t) = \lambda_2^2(\lambda_2 + 3\lambda_1) \\ &M_1 = M_1(t) = \lambda_1^2\lambda_2\Delta t; \quad M_2 = M_2(t) = -\lambda_1\lambda_2^2\Delta t \end{aligned} \tag{8}$$

in which $\lambda_1 = \frac{t_{n+1}-t}{\Delta t}$, $\lambda_2 = \frac{t-t_n}{\Delta t}$.

The global nodal values $\mathbf{v}_n$ of the temporal derivative of temperature at arbitrary time $t \in [t_n, t_{n+1}]$ is interpolated as an independent variable by linear (P1) time shape functions as

$$\mathbf{v}(t) = \mathbf{v}_n^+ \lambda_1(t) + \mathbf{v}_{n+1}^- \lambda_2(t) \tag{9}$$

or simply expressed as

$$\mathbf{v} = \mathbf{v}_n\lambda_1 + \mathbf{v}_{n+1}\lambda_2 \tag{10}$$

As the global nodal values of temperature and its time-derivative vary independently in the following variational equation in the time domain $t \in [t_n, t_{n+1}]$, Eq. (3) is re-expressed as

$$\mathbf{M}\dot{\mathbf{v}} + \mathbf{C}\mathbf{v} + \mathbf{K}\mathbf{T} = \mathbf{Q} \tag{11}$$

with the constraint condition

$$\dot{\mathbf{T}} - \mathbf{v} = \mathbf{0} \tag{12}$$

The weak forms of the semi-discretized equation (11) and the constraint condition (12), together along with the discontinuity conditions of $\mathbf{T}$ and $\mathbf{v}$ on a typical time sub-domain I_n can be expressed by

$$\begin{aligned} &\int_{I_n} \delta\mathbf{v}^{\mathrm{T}}(\mathbf{M}\dot{\mathbf{v}} + \mathbf{C}\mathbf{v} + \mathbf{K}\mathbf{T} - \mathbf{Q})\mathrm{d}t + \int_{I_n} \delta\mathbf{T}^{\mathrm{T}}\mathbf{K}(\dot{\mathbf{T}} - \mathbf{v})\mathrm{d}t \\ &\quad + \delta\mathbf{T}_n^{\mathrm{T}}\mathbf{K}[[\mathbf{T}_n]] + \delta\mathbf{v}_n^{\mathrm{T}}\mathbf{M}[[\mathbf{v}_n]] = 0 \end{aligned} \tag{13}$$

Substituting Eqs. (8)–(10) into Eq. (13), we obtain the following matrix equation from independent variations of $\delta\mathbf{T}_n$, $\delta\mathbf{T}_{n+1}$, $\delta\mathbf{v}_n$, $\delta\mathbf{v}_{n+1}$

$$\begin{bmatrix} \frac{1}{2}\mathbf{K} & \frac{1}{2}\mathbf{K} & -\frac{\Delta t}{4}\mathbf{K} & -\frac{\Delta t}{4}\mathbf{K} \\ -\frac{1}{2}\mathbf{K} & \frac{1}{2}\mathbf{K} & -\frac{\Delta t}{4}\mathbf{K} & -\frac{\Delta t}{4}\mathbf{K} \\ \frac{\Delta t}{4}\mathbf{K} & \frac{\Delta t}{4}\mathbf{K} & \frac{1}{2}\mathbf{M} + \frac{\Delta t}{3}\mathbf{C} & \frac{1}{2}\mathbf{M} + \frac{\Delta t}{6}\mathbf{C} - \frac{\Delta t^2}{12}\mathbf{K} \\ \frac{\Delta t}{4}\mathbf{K} & \frac{\Delta t}{4}\mathbf{K} & -\frac{1}{2}\mathbf{M} + \frac{\Delta t}{6}\mathbf{C} + \frac{\Delta t^2}{12}\mathbf{K} & \frac{1}{2}\mathbf{M} + \frac{\Delta t}{3}\mathbf{C} \end{bmatrix} \times \begin{Bmatrix} \mathbf{T}_n \\ \mathbf{T}_{n+1} \\ \mathbf{v}_n \\ \mathbf{v}_{n+1} \end{Bmatrix} = \begin{Bmatrix} \mathbf{K}\mathbf{T}_n^- \\ \mathbf{0} \\ \mathbf{Q}_1 + \mathbf{M}\mathbf{v}_n^- \\ \mathbf{Q}_2 \end{Bmatrix} \tag{14}$$

where

$$\mathbf{Q}_1 = \int_{I_n} \lambda_1\mathbf{Q}(t)\mathrm{d}t; \quad \mathbf{Q}_2 = \int_{I_n} \lambda_2\mathbf{Q}(t)\mathrm{d}t \tag{15}$$

$$\mathbf{Q}(t) = \mathbf{Q}(t_n)\lambda_1 + \mathbf{Q}(t_{n+1})\lambda_2 = \mathbf{Q}_n\lambda_1 + \mathbf{Q}_{n+1}\lambda_2 \tag{16}$$

Substitution of expression (16) into expression (15) gives

$$\mathbf{Q}_1 = \frac{\Delta t}{3}\mathbf{Q}_n + \frac{\Delta t}{6}\mathbf{Q}_{n+1}; \quad \mathbf{Q}_2 = \frac{\Delta t}{6}\mathbf{Q}_n + \frac{\Delta t}{3}\mathbf{Q}_{n+1} \tag{17}$$

Eq. (14) can be further recast into the following form:

$$\begin{bmatrix} \mathbf{K} & \mathbf{0} & \mathbf{0} & \mathbf{0} \\ \mathbf{0} & \mathbf{K} & -\frac{\Delta t}{2}\mathbf{K} & -\frac{\Delta t}{2}\mathbf{K} \\ \mathbf{0} & \mathbf{0} & \mathbf{M} + \frac{\Delta t}{6}\mathbf{C} - \frac{\Delta t^2}{12}\mathbf{K} & -\frac{\Delta t}{6}\mathbf{C} - \frac{\Delta t^2}{12}\mathbf{K} \\ \mathbf{0} & \mathbf{0} & \frac{\Delta t}{2}\mathbf{C} + \frac{\Delta t^2}{3}\mathbf{K} & \mathbf{M} + \frac{\Delta t}{2}\mathbf{C} + \frac{\Delta t^2}{6}\mathbf{K} \end{bmatrix} \begin{Bmatrix} \mathbf{T}_n \\ \mathbf{T}_{n+1} \\ \mathbf{v}_n \\ \mathbf{v}_{n+1} \end{Bmatrix} = \begin{Bmatrix} \mathbf{K}\mathbf{T}_n^- \\ \mathbf{K}\mathbf{T}_n^- \\ \mathbf{Q}_1 - \mathbf{Q}_2 + \mathbf{M}\mathbf{v}_n^- \\ \mathbf{Q}_1 + \mathbf{Q}_2 + \mathbf{M}\mathbf{v}_n^- - \Delta t\mathbf{K}\mathbf{T}_n^- \end{Bmatrix} \tag{18}$$

This is the basic matrix equation of the time discontinuous Galerkin finite element method (DGFEM). The solutions for nodal temperature vectors $\mathbf{T}_n$, $\mathbf{T}_{n+1}$ are uncoupled from those for nodal derivative vectors $\mathbf{v}_n$, $\mathbf{v}_{n+1}$. Eq. (18) can be further written as

$$\mathbf{T}_n = \mathbf{T}_n^- \quad (\text{that is } \mathbf{T}_n^+ = \mathbf{T}_n^-) \tag{19}$$

$$\begin{bmatrix} \mathbf{M}+\frac{\Delta t}{6}\mathbf{C}-\frac{\Delta t^2}{12}\mathbf{K} & -\frac{\Delta t}{6}\mathbf{C}-\frac{\Delta t^2}{12}\mathbf{K} \\ \frac{\Delta t}{2}\mathbf{C}+\frac{\Delta t^2}{3}\mathbf{K} & \mathbf{M}+\frac{\Delta t}{2}\mathbf{C}+\frac{\Delta t^2}{6}\mathbf{K} \end{bmatrix} \begin{Bmatrix} \mathbf{v}_n \\ \mathbf{v}_{n+1} \end{Bmatrix} = \begin{Bmatrix} \mathbf{Q}_1-\mathbf{Q}_2+\mathbf{M}\mathbf{v}_n^- \\ \mathbf{Q}_1+\mathbf{Q}_2+\mathbf{M}\mathbf{v}_n^- - \Delta t\mathbf{K}\mathbf{T}_n^- \end{Bmatrix} \tag{20}$$

$$\mathbf{T}_{n+1}=\mathbf{T}_n^- + \frac{1}{2}\Delta t(\mathbf{v}_n+\mathbf{v}_{n+1}) \tag{21}$$

It is remarked that continuity of the nodal temperature vector $\mathbf{T}_n$ at any time level t_n in the time domain $I=(0,T)$ is automatically ensured in the present DGFEM formulation. It is only the nodal derivative vectors at discretized time levels that remain discontinuous.

3. Numerical examples for heat wave propagation problems

In this section three numerical examples are employed to demonstrate the validity of the proposed DGFEM in modelling heat wave propagation problems in the media subjected to fast heat impulse.

As the first example we consider a one-dimensional spindly column with length equal to 1 m and subjected to the following initial-boundary conditions:

$$\text{For } x=0: \quad Q=0.5$$

$$\text{For } x=1: \quad T=0$$

$$\text{For } T(x,0)=0 \quad \text{and} \quad \frac{\partial T(x,0)}{\partial x}=0$$

The relaxation time $\tau_0 = 1$ s and thermal diffusivity $a=1$ are taken. Two finite element meshes with different mesh densities of 20×1 and 10×1 four-noded isoparametric elements are considered. The time step is chosen as $\Delta t = 1.0^{-4}$ s. Comparisons of the temperature distributions along the axis of the column at different time levels $t=0.2, 0.5, 1$ s obtained by using the two different mesh densities are illustrated in Fig. 1, which also gives a comparison between the analytical solution [11] and the results given by the present DGFEM.

$$T(x,t)=\int_0^t \sum_{n=1}^{\infty} \frac{1}{\gamma_n} \mathrm{e}^{-[(t-\tau)/2\tau_0]} \sin\frac{n\pi x}{2} \sin\frac{n\pi}{2} \sin\gamma_n(t-\tau)\mathrm{d}\tau \tag{22}$$

in which

$$\gamma_n = \frac{1}{2\tau_0}\sqrt{4\tau_0^2\left(\frac{n\pi a}{2}\right)^2-1}$$

It is observed that the results given by the present DGFEM agree well with the analytical solution. In addition, it is shown that the results obtained for the two different meshes agree to each other very well, therefore, illustrate the good convergence of the proposed DGFEM in the space domain as the finite element mesh is refined.

To demonstrate the performance of the proposed DGFEM in filtering out the spurious numerical oscillations as compared with CGFEM, as the second example, we consider the column with the length equal to 0.2 m subjected to an impulse heat flow flux (see Fig. 2) at the left end ($x=0$) of the column. The essential boundary condi-

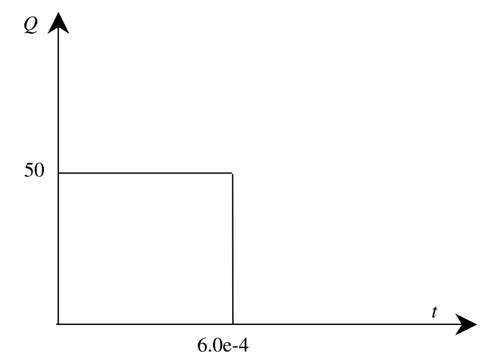

Fig. 2. The impulse heating history for the second example.

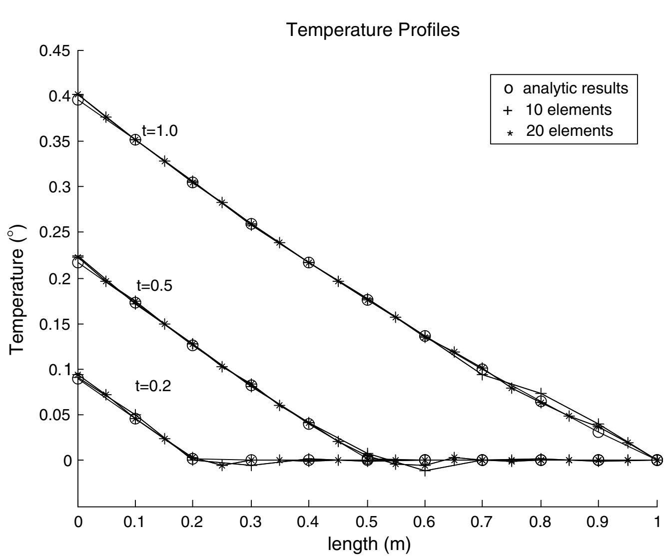

Fig. 1. Instantaneous temperature profiles at different time levels for the two meshes.

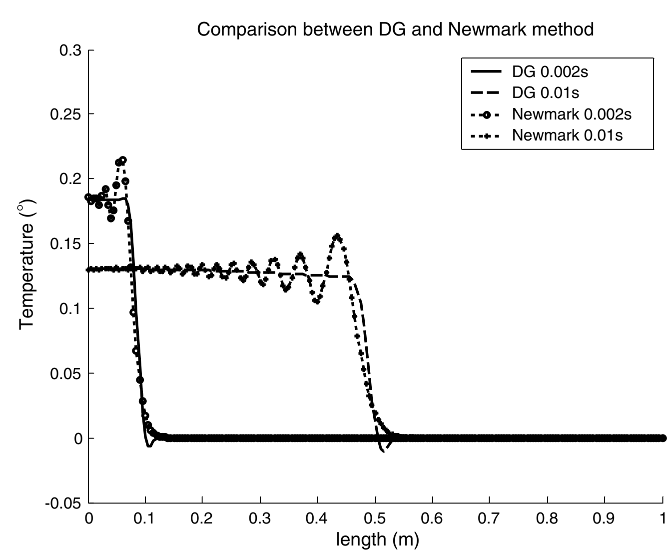

Fig. 3. Instantaneous temperature profiles at different time levels for the two methods.

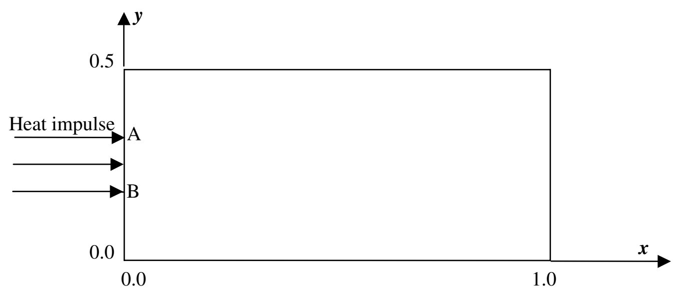

Fig. 4. Geometry for the two-dimensional problem subjected to heat impulse.

tion $T = 0$ is enforced at the right end ($x = 0.2$) of the column. The silent initial conditions, i.e. $T(x, 0) = 0$ and $\frac{\partial T(x,0)}{\partial x} = 0$, are specified over the whole length of the column.

The column is discretized in a 200×1 homogeneous element mesh. The relaxation time $\tau_0 = 0.0001$ s and thermal diffusivity $a = 1$ are used. Fig. 3 illustrates the temperature distributions at the two time levels $t = 0.002, 0.01$ s for the example using the proposed DGFEM and the existing CGFEM with the time step size $\Delta t = 2.0 \times 10^{-4}$ s. The results given in Fig. 3 also demonstrate much better

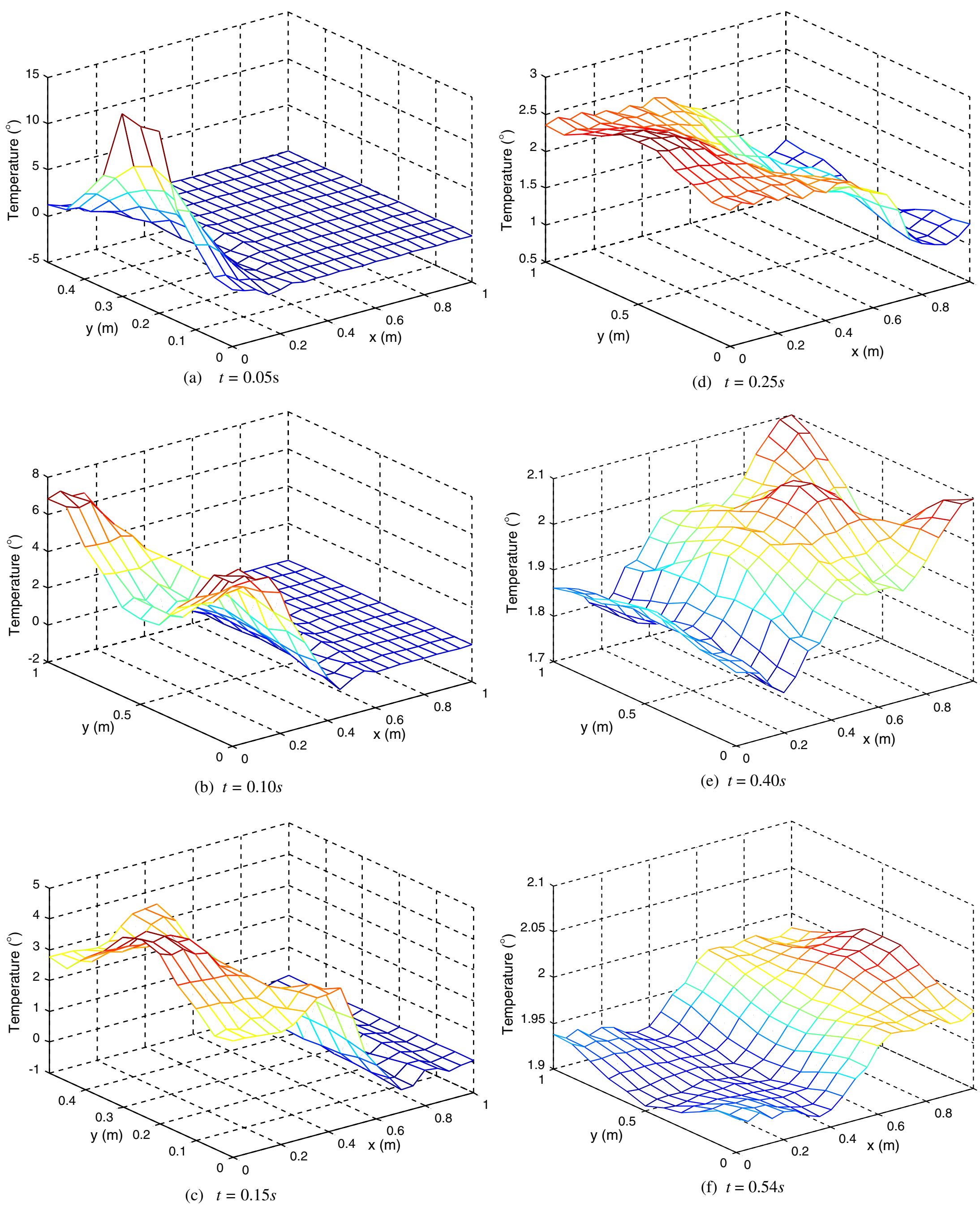

Fig. 5. Three-dimensional maps for temperature distributions in different time levels.

performance of the proposed DGFEM than that of CGFEM in filtering out the spurious numerical oscillation.

To test the performance of the present DGFEM in modelling 2-D heat wave propagation problems, a 2-D problem with the domain $0 \leqslant x \leqslant 1$ m, $0 \leqslant y \leqslant 0.5$ m discretized into a homogeneous 20×10 four-node isoparametric element mesh ($\Delta x = \Delta y = 0.05$) shown in Fig. 4 is considered. The initial temperature over the domain is set to zero. An impulse heat action $Q = 1$ lasting 0.05 s is applied to the middle part AB between $y = 0.2$–0.3 m of the left boundary. The other boundaries are assumed as adiabatic. The relaxation time $\tau_0 = 0.05$ s is taken. The time step is chosen as $\Delta t = 1.0 \times 10^{-4}$ s. The three-dimensional temperature maps at different time levels are illustrated in Fig. 5.

It is observed from Fig. 5a that the temperature level at the zone near the boundary AB, where the heat source is applied, at time $t = 0.05$ s. is higher than that of the zone of the domain far from the boundary AB. Fig. 5b–f demonstrates the heat wave propagation process within the domain at a series of discrete time levels $t = 0.1, 0.15, 0.25, 0.4, 0.54$ s. The convection–diffusion character of the heat wave propagation in the two directions along the x and the y axes can be clearly observed.

4. Conclusion

The present DGFEM characterized by the semi-discrete procedure in spatial domain combined with discontinuous Galerkin interpolation approximation in time domain can effectively capture discontinuities or sharp gradients of the solution for the heat wave problems subjected to heat impulse. The main distinct characteristic of the proposed DGFEM formulations is that the specific P3–P1 interpolation approximations, which uses piecewise cubic and linear interpolations for both temperature and its derivative in the time domain, respectively. Consequently, continuity of the temperature at each discrete time instant is automatically ensured, whereas discontinuity of the derivative of temperature at the discrete time levels still remains.

Comparison with traditional time-stepping algorithms, such as Newmark family algorithm or the γ-family algorithm, the present DGFEM can filter out the effects of the spurious high modes and then the spurious numerical oscillation successfully, in addition, allows large time step sizes to be used due to its three-order accuracy in the time domain [12].

Acknowledgement

The authors are pleased to acknowledge the support for this work by the National Natural Science Foundation of China through grant numbers 10302005, 50278012, 10272027, 10225212, 10421002 and 10590354, the National Key Basic Research and Development Program (973 Program) through contract number 2002CB412709, the Program for Changjiang Scholars and Innovative Research Team in University of China (PCSIRT).

References

[1] X.K. Li, D.M. Yao, R.W. Lewis, A discontinuous Galerkin finite element method for dynamic and wave propagation problems in nonlinear solids and saturated porous media, Int. J. Numer. Meth. Eng. 57 (2003) 1775–1800.

[2] C. Cattaneo, A form of heat conduction equation which eliminates the paradox of instantaneous propagation, Compute Rendus 247 (1958) 431–433.

[3] P. Vernotte, Les paradoxes de la theorie continue de l'equation de la chaleur, Compute Rendus 246 (1958) 3154–3155.

[4] P. Duhamel, Application of a new finite integral transform method to the wave model of conduction, Int. J. Heat Mass Transfer 47 (2004) 573–588.

[5] J. Casas-Vazquez, D. Jou, Nonequilibrium temperature versus local-equilibrium temperature, Phys. Rev. E 49 (1994) 1040–1048.

[6] Q.M. Fan, W.Q. Lu, A new numerical method to simulate the non-Fourier heat conduction in a single-phase medium, Int. J. Heat Mass Transfer 45 (2002) 2815–2821.

[7] M. Honner, Heat wave simulations, Comput. Math. Appl. 38 (1999) 233–243.

[8] K.K. Tamma, R.R. Namburu, Computational approaches with applications to non-classical and classical thermomechanical problems, Appl. Mech. Rev. 50 (1997) 514–551.

[9] K.K. Tamma, X. Zhou, D. Sha, Transient algorithms for heat transfer: general developments and approaches for theoretically generating *N*th-order time-accurate operators including practically useful second-order forms, Int. J. Numer. Meth. Eng. 44 (1999) 1545–1572.

[10] K.K. Tamma, X. Zhou, R. Valasutean, Computational algorithms for transient analysis: the burden of weight and consequences towards formalizing discrete numerically assigned [DNA] algorithmic markers: Wp-family, Comput. Meth. Appl. Mech. Eng. (1997) 149–153.

[11] L.Q. Wang, Solution structure of hyperbolic heat-conduction equation, Int. J. Heat Mass Transfer 43 (2000) 365–373.

[12] X.D. Li, N.E. Wiberg, Structural dynamic analysis by a time-discontinuous Galerkin finite element method, Int. J. Numer. Meth. Eng. 39 (1996) 2131–2152.